Plant Physiol. (1988) 88, 0574–0580
0032-0889/88/88/0574/07/$01.00/0

Do Woody Plants Operate Near the Point of Catastrophic Xylem Dysfunction Caused by Dynamic Water Stress?[1]

ANSWERS FROM A MODEL

Received for publication February 5, 1988 and in revised form May 20, 1988

MELVIN T. TYREE* AND JOHN S. SPERRY
Department of Botany, University of Vermont, Burlington, Vermont 05405

ABSTRACT

We discuss the relationship between the dynamically changing tension gradients required to move water rapidly through the xylem conduits of plants and the proportion of conduits lost through embolism as a result of water tension. We consider the implications of this relationship to the water relations of trees. We have compiled quantitative data on the water relations, hydraulic architecture and vulnerability of embolism of four widely different species: *Rhizophora mangle, Cassipourea elliptica, Acer saccharum,* and *Thuja occidentalis.* Using these data, we modeled the dynamics of water flow and xylem blockage for these species. The model is specifically focused on the conditions required to generate 'runaway embolism,' whereby the blockage of xylem conduits through embolism leads to reduced hydraulic conductance causing increased tension in the remaining vessels and generating more tension in a vicious circle. The model predicted that all species operate near the point of catastrophic xylem failure due to dynamic water stress. The model supports Zimmermann's plant segmentation hypothesis. Zimmermann suggested that plants are designed hydraulically to sacrifice highly vulnerable minor branches and thus improve the water balance of remaining parts. The model results are discussed in terms of the morphology, hydraulic architecture, eco-physiology, and evolution of woody plants.

Transpiration at the leaf surface *pulls* water up from the soil into the roots and through the xylem conduits of plants. Water in xylem conduits is under tension, *i.e.* the xylem pressure potential is negative. This tension increases as soil moisture decreases and/or as transpiration rate increases.

Water under tension can lead to xylem dysfunction by the related processes of cavitation and embolism. Cavitation is the breaking of water continuity in the lumina of xylem conduits (tracheids and vessels) or other cells (*e.g.* fibers) in which water is under tension. There is increasing evidence that cavitations occur when air is sucked into the lumen through a pore in the wall (usually the intervascular pit membrane in xylem conduits) (2, 19, 20). The cavitated lumen is initially filled with water vapor and some air at subatmospheric pressure but soon becomes embolized as it fills entirely with air coming out of solution from surrounding tissue. The shock wave resulting from a rapid (about 1 μs) cavitation event can be detected acoustically in the audio frequency range (9, 10) and in the ultrasonic frequency range (22, 25). Embolism can be measured by how much it reduces the hydraulic conductivity of the xylem.

There is ample evidence to indicate that cavitations induced by drought or excessive transpiration are common events in vascular plants (1–4, 8–12, 14–16, 22, 24, 26, 28). Transpiration in plants is a necessary consequence of the plant's need to maintain rapid gas exchange in leaves for photosynthesis. If plants are to maintain a favorable water balance, efficient channels of water transport must be maintained in the xylem so that water flow from the roots to leaves can replace water lost by transpiration. Embolism can cause a substantial reduction in xylem transport and thus exerts a debilitating influence on the plants water status. There is evidence that embolized conduits can become functional again through bubble dissolution or expulsion. This appears to require a positive xylem pressure potential arising from some mechanism of root or stem pressurization (18, 19). Although there is some evidence for the generation of root pressure nightly in corn during a drought cycle (26), we know of no evidence that this can occur in woody plants. So embolisms may be viewed as irreversible during a critical drought cycle in trees.

The vulnerability of several woody species to cavitation and embolism has been measured. Vulnerability 'curves' show either the cumulative number of cavitation events detected acoustically or the percent loss of hydraulic conductance versus the stem water potential (Ψ[2]) attained during a dehydration. Although acoustic vulnerability curves are easier to measure, they are ambiguous because acoustic signals from large conduits, small conduits, and wood fibers are too similar to distinguish (MT Tyree, JS Sperry, unpublished observations). Hydraulic vulnerability curves are a much more meaningful measure of the impact of embolism on the water relations of plants.

The hydraulic vulnerability curves for four species reported in other papers are redrawn in Figure 1. The lines drawn are trends in the data points for four diverse species: *Rhizophora mangle*, a salt excluding mangrove Rhizophoraceae; *Cassipourea elliptica*, a tropical moist-forest Rhizophoraceae (20); *Acer saccharum*, a temperate hardwood; and *Thuja occidentalis*, a temperate softwood (23). *Rhizophora* is the least vulnerable as suits the demands of its habitat; it grows in sea water and rarely experience Ψs less negative than −2.3 MPa. In April 1987 *Rhizophora* near Miami, Florida never fell below −4.0 MPa (20). In contrast, the other species rarely experience Ψs more negative than −2.0 MPa for *Acer*, −1.8 for *Thuja* and −1.6 for *Cassipourea*.

A cursory evaluation of Figure 1 might lead us to conclude that stem embolisms do not occur to any significant extent in

[1] Various parts of this research were funded by: Natural Sciences and Engineering Research Council of Canada, grant No. A6919, U.S. Department of Agriculture grant No. 86-FSTY-9-0226 and U.S. Department of Agriculture grant No. 85-CRSR-2-2564. Foreign travel costs were covered by Visiting Fellowships to both authors from the Smithsonian Tropical Research Institute and by a grant from the Lintilhac Foundation.

[2] Abbreviations: Ψ, water potential; *E*, evaporative flux; LSC, leaf specific conductivity; CV, coefficient of variation.

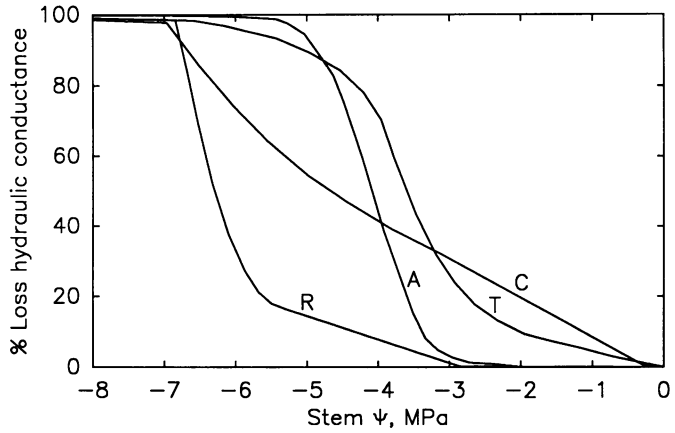

FIG. 1. Vulnerability curves for *Rhizophora* (R), *Acer* (A), *Thuja* (T), and *Cassipourea* (C). These curves are from hand-drawn trends through data sets published elsewhere (25, 27).

any of these species. To achieve a loss of conductance >95% all species must reach stem Ψs of <−6 MPa. Whereas the curves would suggest that all these species would experience less than 15% loss of conductance by embolism at the most negative Ψs commonly found in their habitat. We will argue in this paper that such a cursory examination of these data is misleading and that all these species operate near the point of catastrophic xylem dysfunction caused by dynamic water stress.

All the vulnerability curves in Figure 1 were obtained by a slow dehydration of excised shoots; the Ψs achieved were quasistatic. In nature much of the negative Ψs are achieved dynamically, *i.e.* they arise because of rapid water flow through the stems and the substantial hydraulic resistance encountered. The distinction between dynamic and static stresses has to do with this water flow. If transpiration stops in a plant growing in a field, then stem Ψs will usually rise to a much less negative Ψ, *i.e.* that of the soil. Static stresses remain even when there is no water flow. For example, we knew that the stresses in our slowly dehydrating excised shoots were nearly static because if we reduced flow by reducing the rate of evaporation, stem Ψs did not rise much; little of the drop in Ψ along the stem was due to hydraulic resistance.

Loss of hydraulic conductance from embolism could enhance dynamic water stress by causing a faster flow and thus steeper Ψ gradients in remaining conduits. If total transpiration (and thus total water flow) were constant while cavitations were occurring, the blockage of xylem conduits would force faster transport in the remainder, causing yet more xylem vessels to be blocked by cavitation in a runaway vicious cycle of embolism. We call this cycle of dynamic stress leading to reduced conductance and further dynamic stress an 'embolism cycle.' It is very important to know in theory whether an embolism cycle is inherently unstable. Once started will it lead to runaway embolism and catastrophic dysfunction of the xylem? Or will the cycle lead to a theoretically stable state of reduced hydraulic conductance without further decline in Ψ? If an embolism cycle is inherently unstable, how close to the theoretical limit do trees operate? Has the mechanism of stomatal closure evolved to bring trees up to the brink of catastrophic failure? Optimization theories regarding the cost of carbon allocation to stems and leaves *versus* the payoff in net assimilation would suggest that an optimization bringing trees to the theoretical limit of catastrophic xylem dysfunction may have occurred in species with very different hydraulic architectures (7, 13).

In this paper we present quantitative data on the water relations and hydraulic architecture of the four species in Figure 1 and use a mathematical model of the dynamics of water flow through these trees to answer the questions raised above.

MATERIALS AND METHODS

We studied *Cassipourea elliptica* (Sw.) Poir. (Rhizophoraceae) from the fresh water lake shore of Barro Colorado Island, in Central Panama in the dry season (February) and in the wet season (September) 1987. *Rhizophora mangle* L. (Rhizophoraceae) was studied from the salt water mangrove swamps at the Fairchild Tropical Garden, Miami, FL in April 1987. *Acer saccharum* Marsh. was sampled from Northern Vermont in the summers of 1986 and 1987. *Thuja occidentalis* L. samples were studied on Snake Island, Lake Simcoe about 80 km north of Toronto, Canada in the summers of 1982 and 1985.

Field measurements of shoot Ψ were made periodically with a pressure bomb. Evaporative fluxes (E in kg m^{-2} s^{-1}) and leaf conductances were measured with steady state porometers. These measurements were carried out for many days for *Thuja* and *Acer*. Work on *Cassipourea* and *Rhizophora* was conducted during brief and very busy expeditions so the amount of field work conducted was much less. The objective of these measurements was to obtain estimates of the most likely extreme values for Ψ and E in the 'native' state.

The computer model described in detail below was written to compute, for an assigned value of evaporative flux, the water flow rate, Ψ, and embolism in contiguous segments in a representative branch from each species. A branch or small tree (for *Thuja*) for each species was selected and cut into several hundred numbered segments and cataloged to create the data set for a hydraulic map consisting of a branched catena of segments. Economy in program writing and execution was achieved by numbering the segments starting at the base (segment number 1) and proceeding to side branch segments before proceeding to continuation segments.

Data collected for each numbered segment were: (a) A connecting segment code number. This was the number (N) of the next most basal segment. This was written as $+N$ if two segments were on the same branch, and was written as $-N$ if the next most basal segment was a separate branch. The numbering system on an 11 segment branch is illustrated in Figure 2. (b) The basal diameter of the segment. (c) The length of the segment. Segment lengths were generally cut to lengths less than 10 cm. If there were no side branches and the segment did not taper much, then longer lengths were cut. Generally, segments were cut to lengths that placed the branch insertions near the center of the segment. (d) The surface area of all 'leaves' attached to the segment. Minor

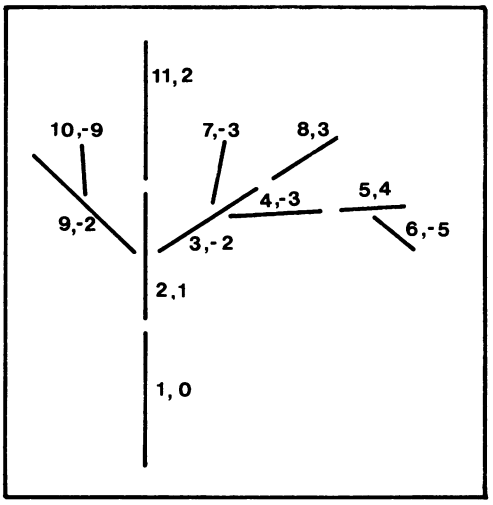

FIG. 2. An illustration of the numbering system used in an 11-segment branch. Places where the branch was cut into segments are indicated by gaps. The first number beside each segment is the segment number, and the second number is the connecting segment number.

side branches less than 3 cm long were treated as connecting leaves and were not cataloged as separate branches.

We assigned each mapped segment with a hydraulic conductance on the basis of empirically derived correlation between stem diameter and hydraulic conductance. Representative stem segments of various diameters were excised from trees. The segments were cut to be >3 times longer than the longest xylem conduits in each species, except *Cassipourea* which had a small percentage (<2%) of very long vessels (2 m or more). The segments were brought into the laboratory, placed under water, and segments successively cut off each end to relieve xylem tensions and remove emboli induced in the ends by excision in the field. For all species except *Thuja* the native embolism was reversed and the maximum hydraulic conductance measured by methods described elsewhere (17). The conductance values (k_h) measured were:

$$k_h = v/(dP/dl) \quad (1)$$

where v = the flow rate (kg s^{-1}) and dP/dl = the pressure gradient (MPa m^{-1}) causing the flow. The *Thuja* conductivity values were collected for a previous publication (27) and are reproduced here in a different format. These conductivity values were not maximum values, *i.e.* the stems probably contained some embolism. Subsequent work has indicated that the loss of hydraulic conductance under field conditions was likely to be about 10% on segments <0.3 cm diameter (22) and conductance values were increased by this amount prior to use in our model.

THE MODEL

A program was written in Turbo Pascal that computed the Ψ of each mapped segment for assigned rates of steady state evaporation. Data needed for a solution in addition to the hydraulic maps were: the appropriate vulnerability curve in Figure 1, soil Ψ, root and bole resistance to water flow, and E. The sequence of program steps were as below:

1. Load data for hydraulic map and corresponding vulnerability curve from Figure 1. Compute hydraulic conductance values for each stem segment based on stem dimensions. For each segment this conductance equaled k_h/l, where l = the segment length and the k_h was selected for the segment diameter from data described under "Measured Data" in Results.
2. Request input of values for soil Ψ and root and bole resistance. (These values were not measured.)
3. Request input of evaporative flux for all leaves.
4. Calculate values of Ψ for each stem segment assuming the same steady state evaporation flux (kg s^{-1} m^{-2}) from all leaves and no loss of conductance from embolism.
5. Save current values of Ψ for each segment.
6. Compute percent loss of conductance for each segment using vulnerability curve (from Fig. 1) and segment Ψ. Adjust all stem conductance values to reflect the computed embolism.
7. Calculate new values of Ψ for each stem segment assuming the same steady state evaporation flux from all leaves and current values of conductance with losses from embolism.
8. See if there are any segments with >95% loss of conductance from embolism. If there are any new ones, declare them dead and remove their leaf area from the transpiration stream.
9. Compare new segment Ψs to previous values (saved in step 5) and find the largest percent change.
10. Is the largest percent change >0.01%?
    If YES then embolism cycle is not stable so go back to step 5.
    If NO then embolism cycle is stable. Print out various results, *e.g.* Ψ at base of branch, average Ψ of all terminal twigs, % leaf area declared dead because of >95% embolism, etc.
11. Restore all stem segments to maximum conductance values and return to step 3 to request a new evaporative flux value.

The model allowed only for steady state solutions, *i.e.* no account was taken for water storage which would delay the attainment of the most negative steady state Ψs. Nonsteady state models that allowed for water storage in the stem and leaves were run, and it was concluded that water storage did not significantly reduce the attainment of the most negative Ψs in minor twigs. These model results for a 10 m *Thuja* tree will be published elsewhere.

In the model we accounted for the approximate 'nodal' resistances (5, 6, 27, 29) by assigning a nodal resistance value equal to about half the resistance of the stem segment containing the branch insertion.

RESULTS

Measured Data. Stem conductance values (k_h) *versus* stem diameter for *Acer* and *Thuja* are shown in Figure 3. The Y values = log (k_h) and the X values = log (diameter). The linear regression from the *Thuja* data yielded $Y = 2.52\ X - 4.606$ and for *Acer* $Y = 2.64\ X - 3.823$. (The curved line for *Acer* is a second order polynomial fit: $Y = -0.717\ X^2 + 2.867\ X - 3.712$.) These regression equations were used to assign conductance values to stem segments in the hydraulic map. The slopes of the regression plots indicate that the specific conductance ($k_s = k_h$/[stem cross sectional area]) of stem sapwood increases with stem diameter. If the sapwood of all stem segments had the same conduit diameter and the same number of conduits per unit cross sectional area, then k_s would be constant. Since stem cross sectional area is proportional to the diameter squared, the slope of the log-log plot in Figure 3 would be 2.00 if k_s were constant. A slope >2 indicates that the average conduit diameter and/or the number of conduits per unit area increase with increasing stem diameter.

Stem conductance data for *Rhizophora* and *Cassipourea* are shown in Figure 4. Time permitted the determination of k_h of stems only in a limited range of sizes. The size of the circles represent the approximate range of k_h values and diameters for 54 and 48 stem segments of *Cassipourea* and *Rhizophora*, respectively. The lines drawn through the points have slopes of 2.0 and 2.7. This range of slopes represent our guess of the likely extremes of possible values.

Table I shows some of the data derived from branch maps and computed k_h values. The data sets for the hydraulic maps of the four species are far too large to present here but are available to anyone wishing to send Dr. Tyree a 5-¼ inch floppy disk for-

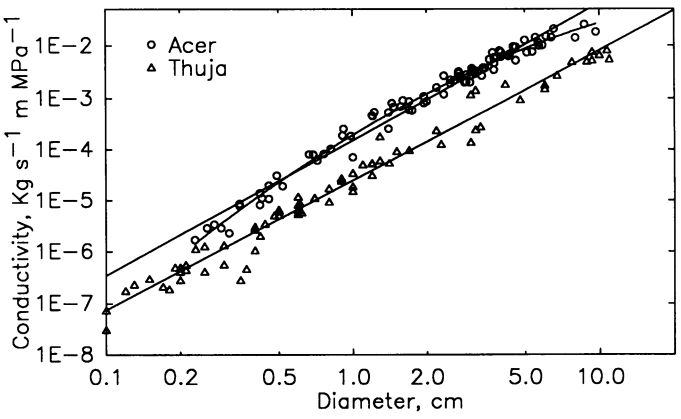

FIG. 3. Stem conductance *versus* stem diameter. For the *Acer* stems we plot maximum conductance after removal of all emboli. For the *Thuja* stems native embolism was not removed. Later work indicated that the native conductances are about 90% maximum.

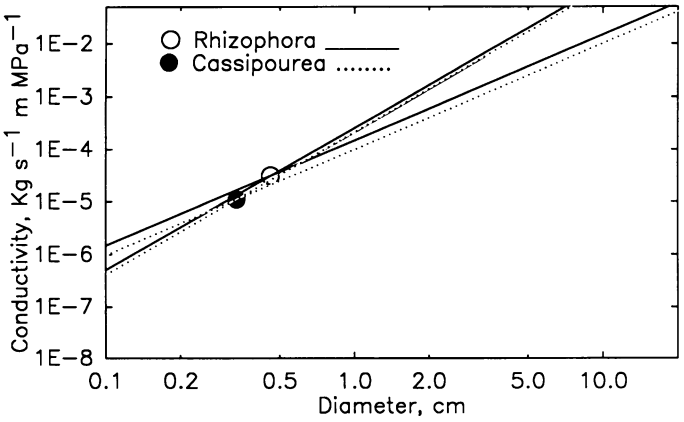

FIG. 4. Stem conductance *versus* stem diameter for *Rhizophora* and *Cassipourea*. See the text for further details.

matted in MS-DOS. The average diameter of segments bearing leaves ranged from a low of 0.102 cm (*Thuja*) to a high of 0.326 cm (*Rhizophora*).

The LSC values in Table I are defined as k_h/(total leaf area fed by the segment) (27). A low LSC indicates that a steep pressure gradient (dP/dl) is needed to maintain the evaporative flux (E) of leaves fed by the stem since $dP/dl = E/\text{LSC}$. The LSC for *Thuja* was calculated on the basis of total evaporative surface area of its scale like leaves whereas the the LSC of other (broad leaf) species was based on the area of only one side of the leaves since stomates were common only on the lower leaf surface of the broad leaf species. But even if the LSC values of *Thuja* are multiplied by a factor of 2.4 (= the ratio of the actual area to projected leaf area) it can be seen that *Thuja* stems are much less capable of supplying water to their leaves than the other species, i.e. the dP/dl needed to maintain an evaporative flux of E in *Thuja* would be about 10 times that required to maintain the same E in the other species.

The Huber values in Table I are equal to the stem cross-sectional area divided by the total evaporative surface area of leaves fed by the stem segment. These values do not differ as much between *Thuja* and the broad leaved trees as does LSC. The Huber values for *Thuja* in minor stems are less than those in the other species, but in major stems the order is reversed. The specific conductivity (k_s) of the sapwood of *Thuja* is about an order of magnitude less than that of the sapwood of the broad leaved species, and that accounts for most of the difference in LSC values between *Thuja* and the other species. This follows because LSC = $k_s \times$ (Huber value).

Others have also found that the LSC of major branches tends to be higher than that of minor branches. This has generally been found to be due to the higher k_s and/or Huber values (5 and 6) in major branches. This pattern is also reflected in our data. In all species, the LSC of basal segments (2.4–3.9 cm diameter) are 4 to 25 times that of the average segment bearing leaves (Table I).

Based on field observations, we present in Table II extreme values of Ψ (most negative) and of E (largest). Note that the largest value of E in *Thuja* is only about one-tenth of that of *Acer* and *Cassipourea* whereas the minimum Ψ values are about the same. These observations are consistent with the lower k_s and LSC values found in *Thuja* (Table I). Apparently, *Thuja* is hydraulically incapable of sustaining the same evaporative flux as the broad leaved species.

Model Results. The model was used to predict the likely extent of embolism of stem segments, and to predict whether the embolism cycle is stable or unstable, leading to catastrophic dysfunction of the xylem due to embolism.

Generally, the model predicted that embolism occurred more in minor than in major branches. The model also predicted that different species could sustain different amounts of embolism in minor shoots and still have a stable embolism cycle. The embolism cycle became unstable and catastrophic xylem dysfunction resulted when the percent loss of hydraulic conductance in minor shoots exceeded about 5% in *Acer*, about 15% in *Thuja* and *Rhizophora*, and about 20 to 30% in *Cassipourea*.; this is about the amount of embolism we have observed in the native state (18, 20). When loss of conductance due to embolism exceeded about 10 to 20% then catastrophic xylem dysfunction resulted.

Table I. *Architecture Data Sets*

The three numbers following the species name are: the number of segments with leaves, the total number of segments in the data set, and maximum path length from base to apex of the stem in m. The row headings are diam., diameter; LSC, leaf specific conductivity kg s^{-1} MPa^{-1} m^{-1}; Huber, Huber value. The column headings are Mean diameter, LSC or Huber value for all segments with leaves; SE, standard error of the mean; CV, coefficient of variance = standard deviation divided by the mean, and base is the diameter, LSC, or Huber value of the basal segment. LSC values for *Cassipourea* and *Rhizophora* were computed using trends for k_h in Figure 4 with slope = 2.7.

Species	Segments with Leaves			Base
	Mean	SE	CV	
Thuja 341, 455, 2.58				
diam.	0.102	0.005	0.931	3.30
LSC	5.45×10^{-6}	4.29×10^{-7}	1.450	1.38×10^{-4}
Huber	4.96×10^{-5}	2.31×10^{-6}	0.861	2.48×10^{-4}
Acer 229, 384, 3.97				
diam.	0.241	0.010	0.618	3.90
LSC	7.28×10^{-5}	6.62×10^{-6}	1.370	8.01×10^{-4}
Huber	1.69×10^{-4}	1.01×10^{-5}	0.905	1.77×10^{-4}
Cassipourea 415, 680, 3.64				
diam.	0.165	0.003	0.309	3.50
LSC	2.46×10^{-4}	1.15×10^{-5}	0.957	1.57×10^{-3}
Huber	3.25×10^{-4}	1.30×10^{-5}	0.815	2.58×10^{-4}
Rhizophora 107, 142, 2.16				
diam.	0.326	0.080	0.248	2.43
LSC	2.77×10^{-4}	1.45×10^{-5}	0.540	1.15×10^{-3}
Huber	2.55×10^{-4}	1.23×10^{-5}	0.510	1.8110^{-4}

Table II. *Extreme Values of E, Evaporative Flux (kg m^{-2} s^{-1}), and of Ψ, Shoot Water Potential (MPa), Observed during Field Observations*

All values are means of a few measurements. The number of observations used for the means is given in brackets.

Species	E	Ψ
Thuja occidentalis	1.8×10^{-5} (3)	−1.8 (3)
Acer saccharum	1.4×10^{-4} (10)	−2.0 (10)
Cassipourea elliptica	2.0×10^{-4} (3)	−1.6 (3)
Rhizophora mangle		−4.0 (2)

The catastrophic xylem dysfunction occurred in a patchwork pattern throughout the minor twigs in the crown, *i.e.* apparently some twigs were more hydraulically favored than others. This results from the large coefficient of variation in LSC values of the segments bearing leaves (Table I). Segments with low LSC values were more prone to catastrophic failure than segments with high LSC values.

Figure 5 summarizes for each species the relationship between assigned value of evaporative flux (E) and a number of computed results including: (a) the Ψ required in the branch segments to maintain the steady state E values and (b) the incidence of catastrophic xylem failure plotted as percent loss of leaf area. Note that the range of values of E differ for each species in Figure 5.

Figure 5a (upper left) shows results for *Thuja*. Soil Ψ is set at 0 MPa. The open circles show the computed average Ψ of all segments bearing leaves when no change in stem conductance from embolism occurs. When embolism develops due to dynamic water stress then the computed average Ψ of all segments bearing leaves is slightly more negative (closed circles for E values $< 2 \times 10^{-5}$) because of the increased hydraulic resistance of embolized stems. But when catastrophic xylem dysfunction occurs because of an unstable embolism cycle, minor branches begin to die leading to an increase in percent loss of leaf area (closed triangles). The loss of leaf area caused a reduction in volume flow rate, v, in the remaining living stems since $v = A_T E$ where A_T is the total area of leaves fed by the stem segment. The reduction in A_T apparently more than offsets the increase in E. The resulting reduction in v causes an improved water balance in the remaining living segments (see closed circles for $E > 2 \times 10^{-5}$) even though E increases. The Ψ at the base of the *Thuja* treelet (open triangles) decreases with increasing E until leaf loss by catastrophic xylem dysfunction. After that the water balance at the root collar improves because the reduction in A_T more than offsets the increase in E so v decreases in the roots. The extreme value of E observed in *Thuja* is indicated by an '*' near the X-axis. Note that if this species had higher E values than catastrophic xylem dysfunction would occur. In this model the root resistance to water flow was adjusted to account for about 18% of the total resistance to water flow from the soil to the leaves. This choice is justified by a more detailed model on a 10 m tree to be published elsewhere, but it is justified also because the model predicts the range of Ψs observed in the field.

About the same relationships are found in the model for *Acer* as that for *Thuja*. In this model the calculations were done for a branch so the root + bole resistance was set to account for about 25% of the overall drop in Ψ from the soil to the leaves. Most of the data plotted (circles and triangles) were based on k_h values calculated from the linear regression in Figure 3. When the second order regression is used (curved line in Fig. 3) the results do not change by much. The percent loss of leaf area for this case is plotted with square symbols.

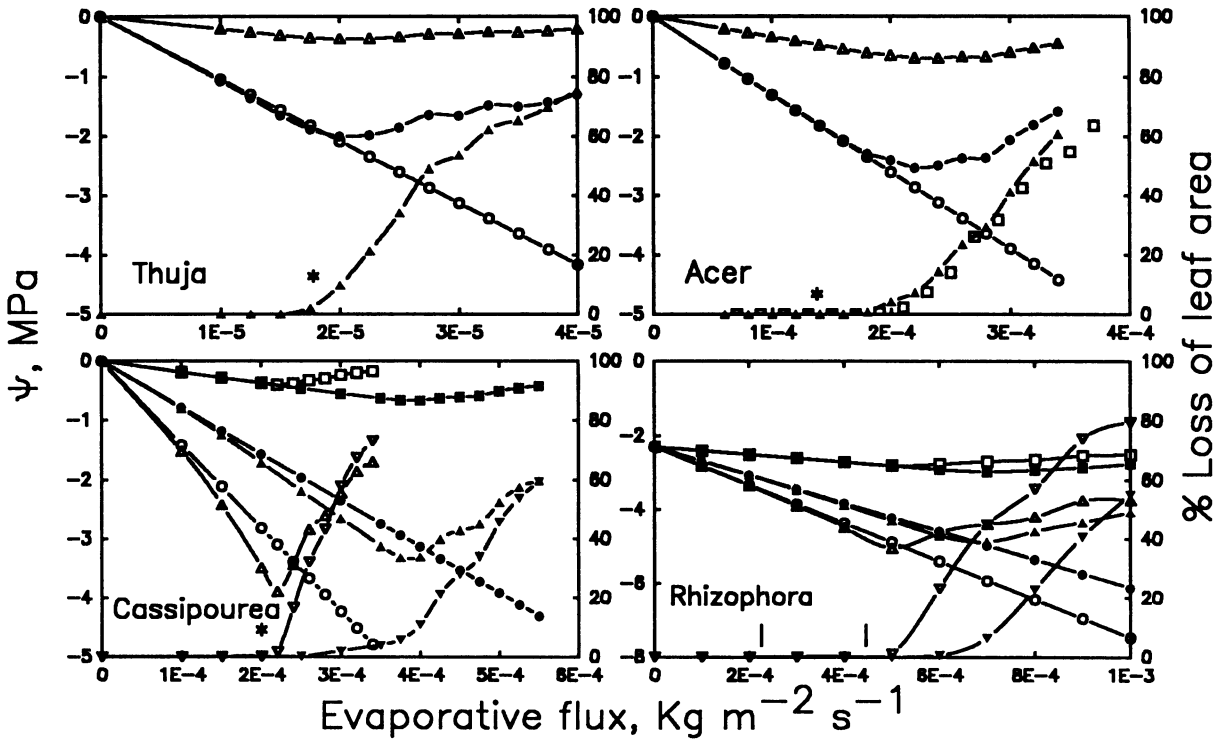

FIG. 5. Results from the model. For *Thuja* and *Acer* we show plots of: Ψ at the base of the small tree or branch (open triangles), the average Ψ of all minor stems bearing leaves assuming no embolism at all (open circles) or if embolism occurred (closed circles). The percent loss of leaf area for each are plotted with closed triangles. The '*' near the X-axis represent the extreme values of evaporative flux (E) observed in field measurements. For *Cassipourea* and *Rhizophora* the model was solved for two cases: (a) When k_h follows the trend in Figure 4 with slope = 2.0 (open symbols) and (b) when k_h follows the trend in Figure 4 with slope = 2.7 (closed symbols). For both tropical species we have: Ψ at the base of the branches (squares), the average Ψ of all minor branches bearing leaves assuming no embolism (circles) and when there is embolism (triangles), and the % loss of leaf area (inverted triangles). See the text for further details.

The model data for *Cassipourea* were calculated for two cases: (a) a slope in Figure 4 of 2.0, which represents constant specific conductance, k_s (open symbols), and (b) a slope in Figure 4 of 2.7, which represents the usual pattern of increasing k_s with increasing stem diameter (closed symbols). In the former case the predicted Ψs were more negative than observed in nature whereas the values resulting from the latter (slope 2.7) yielded about the right values of Ψ.

The model data for *Rhizophora* were calculated like those of *Cassipourea* except that the soil Ψ was set at −2.3 MPa, near that of sea water. No measurement of extreme E were made for *Rhizophora* but the vertical lines close to the X axis give what the extreme value would be under the following conditions: air and leaf temperature, 38°C; RH, 50%; and leaf resistance to vapor diffusion of 1 and 0.5 s cm^{-1} for the left and right ticks, respectively. In *Rhizophora* a believable range of Ψs was predicted when the slope of k_h *versus* stem diameter (Fig. 4) was set at either 2.0 (open symbols) or 2.7 (closed symbols).

In Table III we examined the impact of using different values for the soil Ψ or root and bole resistance on the results of the model. The first entries under each species are the soil Ψ and root and bole resistances used in Figure 5 and the E value at which the model predicts a 10% loss of leaf area by catastrophic xylem dysfunction (symbolized as E10%). The subsequent entries give the E10% values when the soil Ψ or root and bole resistances are changed. Lowering the soil Ψ by 0.8 MPa results in a 17 to 25% decline in E10%. Increasing the root and bole resistance by a factor of 2 results in a decrease in E10% of the 10 to 17%, and decreasing the root and bole resistance by a factor of 2 results in an increase of E10% by 8 to 11%.

Two striking generalizations result from all the models: (a) Although the likely maximum E of all species differ, these maxima are all near the point of catastrophic xylem dysfunction and loss of leaf area caused by embolism during dynamic water stress. (b) After catastrophic failure of selected minor branches, the model predicts an improved water balance (less negative Ψ) due to leaf loss from dead shoots. These results are in accord with Zimmermann's plant segmentation hypothesis (see below).

Table III. *Effect of Changing the Soil Water Potential (Ψ_{soil}, MPa) or Root Resistance (rr, MPa s kg^{-1} m^{-1}) on the Evaporative Flux at Which 10% Leaf Loss (E10%, kg s^{-1} m^{-2}) Occurs*

In each case the first values are those used in Figure 5. The column headed % Change is the percent change in E10% relative to the first entry for each species.

Species	Ψ_{soil}	*rr*	*E*10%	Change
				%
Thuja	0.0	6×10^{3}	2.00×10^{-5}	
	−0.4	6×10^{-3}	1.77×10^{-5}	−11.5
	−0.8	6×10^{3}	1.50×10^{-5}	−25.0
	0.0	12×10^{3}	1.80×10^{-5}	−10.0
	0.0	3×10^{3}	2.16×10^{-5}	8.0
Acer	0.0	5×10^{2}	2.40×10^{-4}	
	−0.4	5×10^{2}	2.17×10^{-4}	−9.5
	−0.8	5×10^{2}	1.95×10^{-4}	−18.8
	0.0	10×10^{2}	2.01×10^{-4}	−16.3
	0.0	2.5×10^{2}	2.66×10^{-4}	10.8
Cassipourea	0.0	5×10^{2}	3.96×10^{-4}	
	−0.4	5×10^{2}	3.58×10^{-4}	−9.6
	−0.8	5×10^{2}	3.28×10^{-4}	−17.2
	0.0	10×10^{2}	3.43×10^{-4}	−13.4
	0.0	2.5×10^{2}	4.33×10^{-4}	9.3
Rhizophora	−2.3	4×10^{2}	7.5×10^{-4}	
	−2.7	4×10^{2}	6.5×10^{-4}	−11.0
	−3.1	4×10^{2}	5.7×10^{-4}	−21.9
	−2.3	8×10^{2}	6.05×10^{-4}	−17.1
	−2.3	2×10^{2}	8.2×10^{-4}	11.2

DISCUSSION

The factor that determines the development of dynamic water stress in stems and the embolism that results from the stress is the rate of water flow, v, through the stems and not E *per se*. So the relationships in Figure 5 can be viewed in a more general sense. The value of v in any segment is E^*A, where A is the area of leaves fed by the segment. So the X-variable in Figure 5 could equally well be A with E constant rather than E with A constant. In that case we would be asking the following question: Could these species increase their competitive advantage by adding more leaves without investing carbon in sapwood? The answer to this ecophysiological (or morphological) question is 'no' because doing so would induce catastrophic xylem failure. The value of E depends on both environmental and biological factors; among the biological factors are: stomatal physiology, stomatal size, and stomatal frequency. So we could ask another question: Could these species increase their net assimilation and competitive advantage through an increase in stomatal size or frequency because that would increase CO_2 uptake? The answer is 'no' because that would also increase E and cause xylem failure.

Zimmermann (29) was the first to put the study of the hydraulic architecture of trees on a quantitative level. He and others (5, 6, 27) have since established two general properties of tree hydraulic architecture: (a) the LSC of minor branches is less than that of major branches and (b) significant resistances to water flow reside in branch insertions. These two factors mean that the overall resistance to water flow from the soil to minor branches are approximately equal regardless of how far the minor branch is from the soil. Without this, branches near the base of trees would be hydraulically favored over branches at the apex. Presumably, if apical branches were unfavored hydraulically they could not grow fast enough to compete for light. In trees with strong morphological apical dominance, LSC values sometime increase toward the dominant apex and decrease toward subdominant apices (5, 6).

These relationships led Zimmermann (30) to propose the plant segmentation hypothesis. He suggested that LSC declines toward most apices and that nodal resistance is significant because both help to confine cavitations and embolism to expendable minor branches. Dicot and gymnosperm trees commit considerable biomass to major stems and palms have no means of replacing the xylem in their stems. So Zimmermann suggested that plant segmentation would contribute to the preservation of these costly or irreplaceable organs and allow trees to survive periods of extreme drought. Our model lends considerable credence to the plant segmentation hypothesis and also a new dimension to the hypothesis. That is, the model predicts a patchwork pattern to the catastrophic loss of minor branches and an improved water balance for the minor branches that survive.

The reason for the patchwork pattern of stem die-back is probably related to the high CV in LSC and Huber values of minor branches. The segments with low LSC will be the first to die-back. The CV for Huber values range from 0.5 to 0.9 and for LSC values range from 0.54 to 1.45. The LSC values in Table I were calculated from population mean values of k_h and not the actual value so the CVs could be overestimated. For stems of a small diameter size class, there is a large CV for k_h (Fig. 3), for k_s, and for leaf area which is reflected directly in the Huber value. If stems in a small diameter class with high leaf area (low Huber value) also have a high k_s then this would tend to reduce the CV in the LSC value. To resolve this question we calculated CV values on directly measured LSC values for some minor branches of *Acer* and *Thuja* and found them to be in the range of 0.8 to 1.0; thus the CVs in Table I were not seriously overestimated. Factors contributing to high variation in LSC values would include leaf loss by herbivory, frost, wind, and other physical damage; and by changes in the relative rates of stem and leaf

growth caused by changes in microenvironment (mostly light level?) from year to year.

It is rare to find individual trees that suffer significant leaf loss due to drought. This is presumably because stomates close and reduce E before catastrophic xylem dysfunction and leaf loss. When we modified our model to account for stomatal closure at leaf Ψs of about -2.0 MPa in *Thuja* and -2.4 MPa in *Acer* then the model did not predict leaf loss by catastrophic xylem dysfunction. The value of the model (without stomatal regulation), is that it shows for the first time that diverse species of trees all operate near the point of catastrophic xylem failure. The only possible exception to this might be *Rhizophora*. We would predict a maximum E around 3×10^{-4} kg m^{-2} s^{-1} which is considerably lower than the value causing severe xylem failure. A high margin of safety might be required because *Rhizophora* may have no mechanism of embolism reversal. We suggest this because *Rhizophora* grows in sea water and excludes salts from the xylem stream (21); consequently, we can not imagine any way that *Rhizophora* could generate root pressure to reverse embolism. We know that *Acer* can reverse embolism in the spring by the generation of root and/or stem pressure (18) and we cannot exclude the possibility that similar mechanisms for embolism reversal might exist for *Thuja* and *Cassipourea*.

We presume that stomatal closure due to water stress will prove to be the first defense against catastrophic xylem dysfunction in woody plants. If so, then one can ask whether a species might improve its competitive advantage of maintaining a low Huber value (more leaf area per unit stem cross-sectional area) and preventing catastrophic xylem dysfunction through stomatal closure for part of the day. Mid-day stomatal closure has been observed in many plants. To answer this question one must weight the extra investment the species must put into leaves *versus* the reduced net assimilation on those days in which stomatal closure is necessary to prevent xylem embolism. Some species appear to sustain E values right at the limit of catastrophic failure, *e.g. Thuja* and *Cassipourea*, whereas others appear to have a larger safety margin, *e.g. Acer* and *Rhizophora* (Fig. 5). We suggest (rather tentatively) that *Acer* is conservative because catastrophic xylem dysfunction occurs after only a very small percent loss of hydraulic conductance compared to the other species, *i.e.* at a 5% loss in *Acer versus* at a >15% loss for the other species; so *Acer* has very little margin for error. We have already discussed the potential reason for conservatism in *Rhizophora* in terms of the presumed inability of *Rhizophora* to repair embolism through root pressure.

Could catastrophic xylem dysfunction be a potential threat for all woody species? If so then this would suggest that there must be a strong selective process for a number of diverse morphological and physiological properties in woody plants that somehow keeps the water relations of the species in proper balance. These morphological features include: leaf area supported per unit stem area (inverse Huber value), stomatal diameter, stomatal frequency (number per unit area), and xylem structure (small *versus* large conduits). One can speculate that xylem structure (*e.g.* tracheids in conifers *versus* vessels in hardwoods) might be much less genetically mutable than the genetics that determines leaf size and number (related to Huber values), stomatal size, stomatal frequency, stomatal physiology. A tree cannot improve its competitive status with regard to competition for light and net assimilation through any process that would increase E without changing the less mutable xylem morphology. Thus, the xylem morphology of conifers appears to constrain these species to leaf morphologies and physiologies that result in low evaporative flux and reduced gas exchange rates in general.

The application of the principles we have learned about the hydraulic architecture of trees and the vulnerability of xylem to embolism could provide new insights into the evolution of the morphology and physiology of woody plants. It could also provide new information about the ecophysiology of woody species. Modeling of these interacting factors could be a powerful tool to understanding the complex interactions entering into these questions.

Acknowledgments—We thank Tim Wilmot for assistance in measuring some hydraulic conductance values and the hydraulic map for *Acer*. We thank John Donnelly for assistance in measuring some hydraulic conductance values of *Rhizophora*. John Donnelly, Bert Leigh, John Raven, and Barry Tomlinson all read and suggested improvements to this manuscript, but are not responsible for any deficiencies that may remain.

LITERATURE CITED

1. Byrne GF, JE Begg, GK Hansen 1977 Cavitation and resistance to water flow in plant roots. Agric Meteorol 18: 21–25
2. Crombie DS, MF Hipkins, JA Milburn 1985 Gas penetration of pit membranes in the xylem of *Rhododendron* as the cause of acoustically detectable sap cavitation. Aust J Plant Physiol 12: 445–453
3. Crombie DS, JA Milburn, MF Hipkins 1985 Maximum sustainable xylem sap tensions in *Rhododendron* and other species. Planta 163: 27–33
4. Dixon MA, J Grace, MT Tyree 1984 Concurrent measurements of stem density, leaf and stem water potential, stomatal conductance and cavitation of a sapling of *Thuja occidentalis* L. Plant Cell Environ 7: 615–618
5. Ewers FW, MH Zimmermann 1984 The hydraulic architecture of balsam firs (*Abies balsamea*). Physiol Plant 60: 940–946
6. Ewers FW, MH Zimmermann 1984 The hydraulic architecture of eastern hemlock (*Tsuga canadensis*). Can J Bot 62: 940–946
7. Givnish, TJ 1986 On the Economy of Plant Form and Function. Cambridge Univ Press, Cambridge
8. Jones HG, J Pena 1986 Relationships between water stress and ultrasound emission in apple. (*Malus* × *domestica* Borkh.). J Exp Bot 37: 1245–1254
9. Milburn JA 1973 Cavitation studies on whole *Ricinus* by acoustic detection. Planta 112: 333–342
10. Milburn JA, RPC Johnson 1966 The conduction of sap. II. Detection of vibrations produced by sap cavitation in *Ricinus* xylem. Planta 66: 43–52
11. Milburn JA, ME Mclaughlin 1974 Studies of cavitation in isolated vascular bundles and whole leaves of *Plantago major* L. New Phytol 73: 861–871
12. Pena J, J Grace 1986 Water relations and ultrasound emissions of *Pinus sylvestris* L. before, during and after a period of water stress. New Phytol 103: 515–524
13. Raven JA, LL Handley 1987 Transport processes and water relations. New Phytol 106(suppl): 217–233
14. Salleo S, MA Logullo 1986 Xylem cavitation in nodes and internodes of whole *Chorisia insignis* H.B. et K. plants subjected to water stress: relations between xylem conduit size and cavitation. Ann Bot 58: 431–441
15. Sperry JS 1985 Xylem embolism in the palm *Rhapis excelsa*. IAWA Bull (NS) 6: 283–292
16. Sperry JS 1986 Relationship of xylem pressure potential, stomatal closure, and shoot morphology in the palm *Rhapis excelsa*. Plant Physiol 80: 110–116
17. Sperry JS, JR Donnelly, MT Tyree 1988 A method for measuring hydraulic conductivity and embolism in xylem. Plant Cell Environ 11: 35–40
18. Sperry JS, JR Donnelly, MT Tyree 1988 Seasonal occurrence of xylem embolism in sugar maple (*Acer saccharum*). Am J Bot 75: 1212–1218
19. Sperry JS, NM Holbrook, MH Zimmermann, MT Tyree 1987 Spring filling of xylem vessels in wild grapevine. Plant Physiol 83: 414–417
20. Sperry JS, MT Tyree, JR Donnelly 1988 Vulnerability of xylem to embolism in two species of Rhizophoraceae. Physiol Plant (in press)
21. Tomlinson PB 1986 The Biology of Mangroves, Chap. 6. Cambridge Univ Press, Cambridge
22. Tyree MT, MA Dixon 1983 Cavitation events in *Thuja occidentalis* L.? Ultrasonic acoustic emissions from the sapwood can be measured. Plant Physiol 72: 1094–1099
23. Tyree MT, MA Dixon 1986 Water stress induced cavitation and embolism in some woody plants. Physiol Plant 66: 397–405
24. Tyree MT, MA Dixon, RG Thompson 1984 Ultrasonic acoustic emissions from the sapwood of *Thuja occidentalis* measured inside a pressure bomb. Plant Physiol 74: 1046–1049
25. Tyree MT, MA Dixon, EL Tyree, R Johnson 1984 Ultrasonic acoustic emissions from the sapwood of cedar and hemlock: an examination of three hypotheses concerning cavitations. Plant Physiol 75: 988–992
26. Tyree MT, EL Fiscus, SD Wullschleger, MA Dixon 1986 Detection of xylem cavitation in corn under field conditions. Plant Physiol 82: 597–599
27. Tyree MT, MED Graham, KE Cooper, LJ Bazos 1983 The hydraulic architecture of *Thuja occidentalis*. Can J Bot 61: 2105–2111
28. West DW, DF Gaff 1976 Xylem cavitation in excised leaves of *Malus sylvestris* Mill. and measurements of leaf water status with the pressure chamber. Planta 129: 15–18
29. Zimmermann MH 1978 Hydraulic architecture of some diffuse-porous trees. Can J Bot 56: 2286–2295
30. Zimmermann MH 1983 Xylem Structure and the Ascent of Sap. Springer, New York